Available online at www.sciencedirect.com
ScienceDirect
International Journal of Heat and Mass Transfer 50 (2007) 117–126
International Journal of HEAT and MASS TRANSFER
www.elsevier.com/locate/ijhmt

Spatial thermal regulation of aluminum foam heat sink using a sintered porous conductive pipe

Sheng-Chung Tzeng *

Department of Mechanical Engineering, Chienkuo Technology University, No. 1, Chieh Shou N Rd., Changhua 500, Taiwan, ROC

Received 4 November 2005; received in revised form 27 June 2006
Available online 1 September 2006

Abstract

The work investigated the spatial thermal regulation of an aluminum foam heat sink using a high-conductivity conductive pipe. The fluid medium was air. The test specimens were measured in four modes – without a conductive pipe (A), with a copper conductive pipe (B), with arc gaps in the front and rear parts of the porous conductive pipe (C) and with lateral arc gaps beside the porous conductive pipe (D). The range of Reynolds numbers was $Re = 883$–4416. Local and average Nusselt numbers were examined. The experimental results indicate that the conductive pipe in an aluminum foam heat sink was very effective in spatial thermal regulation, especially in mode D with lateral arc gaps, which were approximately along the stream-wise axis, beside the conductive pipe. However, using the conductive pipe in the aluminum foam heat sink studied herein did not promote overall heat transfer.

Keywords: Spatial thermal regulation; Porous medium; Heat sink; Heat transfer

1. Introduction

Consumer demand for high-speed and multi-functionality of computers has led to an increase in the circuit density per unit area of chip, and an increased power dissipation per unit volume. Therefore, thermal management is an increasingly important aspect of electronic product design. The random structure and extremely large solid–air contact area of porous material are such that heat sinks made of porous media are expected to satisfy future cooling requirements. Of many porous media, metal foams and sintered metal beads have attracted the attention of numerous researchers, who have studied heat and mass transport in them. Most metal foams are highly porous ($\varepsilon \geqslant 0.9$) and so have a high-permeability ($K = 10^{-8}$–$10^{-7}\,\mathrm{m}^2$). The porosity of sintered metal beads is around 0.4 and the typical magnitude of permeability is $10^{-10}\,\mathrm{m}^2$. Hence, a comparison with sintered porous materials at a given pumping power shows that these metal foams permit more coolant to pass through, carrying more heat away. However, the effective thermal conductivity of sintered metal beads commonly exceeds that of metal foams because of the higher solid fraction and sintered structure, suggesting that sintered metal beads are preferred for transferring heat.

Several interesting works of heat transfer in a channel filled with metal foams [1–6] or sintered metal beads [7–11] have been published. These studies improve our understanding of heat transfer by porous metallic materials. All such works involve a typical inlet flow direction that is parallel to the channel axis, and only porous metallic materials fill the test channels. Recently, porous metallic materials have been used with other cooling technologies (such as inserting metal baffles or fins and using impinging or oscillating flows) to improve further heat transfer. Rizk and Kleinstreuer [12], Ould-Amer et al. [13] and Huang et al. [14] numerically studied the enhancement of forced convection cooling of discrete heated blocks in a channel using porous media. They found that the efficiency of the new configuration was around 50% higher than that of a traditional open-channel cooling system. Bhattacharya and

* Tel.: +886 4 7111111x3132; fax: +886 4 7357193.
E-mail addresses: tsc@ctu.edu.tw, tsc33@ms32.hinet.net

0017-9310/$ - see front matter © 2006 Elsevier Ltd. All rights reserved.
doi:10.1016/j.ijheatmasstransfer.2006.06.034

Nomenclature

D	diameter of the conductive pipe (m)
F	inertial coefficient
H	height of the Al-foam heat sink (m)
K	permeability (m^2)
k	thermal conductivity (W/m K)
L	length of the Al-foam heat sink (m)
Nu	local Nusselt number, $qH/(T_w - T_i)/k_f$
$\overline{Nu}$	average Nusselt number for the whole heat sink, Eq. (5)
$\overline{Nu}_{(y/H=1.4)}$	average Nusselt number at the centerline of the heat sink, Eq. (4)
p	pressure (Pa)
P	non-dimensional pressure drop, $(p_i - p_e)/(0.5\rho_f U_i^2)$
PPI	pore density of the metal foam, pore per inch
q	heat flux (W/m^2)
Re	Reynolds number, $\rho_f UH/\mu$
T	temperature (°C)
U	average fluid velocity (m/s)
W	width of the Al-foam heat sink (m)
x	stream-wise coordinate (m)
y	span-wise coordinate (m)

Greek symbols

ε	porosity
μ	viscosity (kg/m s)
ρ	density (kg/m^3)

Superscript

*	effective

Subscripts

e	at channel exit
f	fluid
i	at channel inlet
w	channel wall

Mahajan [15] embedded longitudinal plate fins in an aluminum foam heat sink and experimentally investigated the heat transfer performance of the cooling system. The fins made of solid aluminum increased the conductive dissipation of heat, and the area of the heated surface in contact with metal foams. They showed that incorporating fins into metal foams markedly increased heat transfer. Tzeng et al. [16] experimentally determined the local and average heat transfer characteristics in asymmetrically heated sintered porous channels with periodical baffles. Measurements are made on the test specimens in four modes – without baffles (A), with periodic baffles on top (B), with periodic baffles on bottom (C) and with staggered periodic baffles on both sides (D). At $Re > 2000$, heat transfer was greatest in mode B and least in mode D, in which the heat transfer was even poorer than that without baffles. At an Re of around 1000, mode D was associated with excellent heat transfer. In that case, heat transfer was enhanced by 20%–30% in mode D, 10%–20% in mode B and 0%–12% in mode Fu and Huang [17,18], Jeng and Tzeng [19] and Tzeng and Jeng [20] examined the heat transfer characteristics of porous heat sinks with an unconfined slot jet, a confined slot jet and a 90° turned flow, respectively, in applications of porous media with impinging flow. An interesting heat transfer distribution was identified. It was influenced by the formation of the recirculation zone adjacent to the jet nozzle. The results reveal that when the Reynolds number is low, the heat transfer was maximal at the stagnation point. However, as the Reynolds number increased, the maximum heat transfer moved downward – to the narrowest part between the recirculation zone and the heating surface. This phenomenon can be exploited in spatial thermal regulation. Another approach of spatial thermal regulation involves the use of oscillating flow. Leong et al. [21–23] studied heat transfer of a porous channel under oscillating flow. They found that the heated surface temperature distribution associated with oscillating flow was convex, with a maximum point at the center of the test section. It differs from the monotonically increasing under steady flow.

This work proposes a new cooling system by embedding a high-conductivity conductive pipe into a metal foam heat sink. Four test modes of the conductive pipes were used. A series of experiments were conducted to elucidate the effect of the conductive pipe configuration on spatial thermal regulation. Local and average Nusselt numbers were investigated. The results are interesting and can be used as a reference for related cooling designs.

2. Experimental apparatus and test section

The experimental setup, presented in Fig. 1, was divided into four main parts – (1) air supply system; (2) test section; (3) test specimens, and (4) data acquisition system. Firstly, the air compressor (MITSUISEIKI 10 HP) blew air into the air tank. Then, the air flowed through a filter to remove the oil, water and particles. Finally, the air entered the test section after it had passed through the straightener, which was made of a mesh screen. The air pressure in the test section was only little higher than the atmospheric pressure because that the test section was positioned near at the end of the experimental system. The air flow rate was controlled using an electric digital mass flow controller (AALBORG GFC771S) within the range 0–1000 l/min. The test section was made of 40 mm-thick Bakelite. The dimensions of the channel section were 60 mm × 21.5 mm. The channel was filled with test specimens of dimensions 60 mm × 21.5 mm × 60 mm. A film heater was fixed to

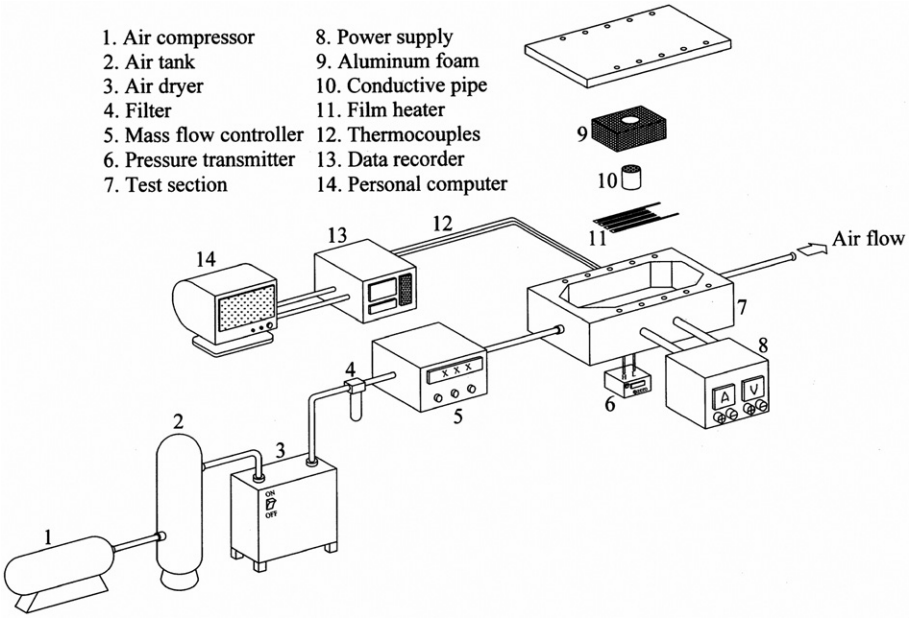

Fig. 1. Experimental apparatus.

the inner surface of the bottom wall of the channel to provide the constant heat flux to the test specimen. The wall heat fluxes supplied to the film heater from the electronic power were 0.88–1.66 W/cm^2 at a flow rate of 50–250 l/min. The other walls of the channel were insulated.

The test specimens were made of aluminum foams, each with a cylindrical cavity, formed using a WEDM (wire electronic discharge machine). A conductive pipe made of copper or sintered bronze beads was inserted into the cavity. The height and the diameter of the conductive pipe were 21.5 mm and 30 mm, respectively. Sufficient highly thermally conductive grease was applied to the contact surfaces among the film heater, the aluminum foams and the conductive pipe, to reduce the thermal contact resistance. Table 1 presents the parameters associated with the porous materials used herein, such as the permeability (K), the inertial coefficient (F), the effective thermal conductivity (k^*) and others. The K and F values were obtained by the method of Hunt and Tien [1]. The value of k^* was measured by performing a number of one-dimensional conduction heat transfer experiments. The test method was presented in Ref. [24]. The configurations of the test specimens were divided into four modes. Mode A was without a conductive pipe; mode B was with a conductive pipe made of the copper, and modes C and D were with conductive pipes made of sintered bronze beads. The conductive pipe made of sintered bronze beads had a 2 mm-thick copper shield to form the cylinder during sintering. Part of the copper shield was cut using a WEDM. In mode C, the gaps in the copper shield of the conductive pipe were at the front and the rear of the cylindrical cavity in the aluminum foam heat sink. The coolant could flow through the conductive pipe because the gaps were in the direction of the stream. In mode D, the same conductive pipe as used in mode C was turned through 90°, and the gaps in the copper shield of the conductive pipe were present on both lateral sides of the cylindrical cavity in the aluminum foam heat sink. The various directions of the gaps yield various flow pattern, suggesting a change in thermal performance. Fig. 2 shows photographs of the test specimens examined herein.

Table 1
Physical properties of porous media

Porous media	Aluminum foam	Sintered bronze beads
Pore density, PPI or average bead diameter, d (mm)	10 PPI	0.7 mm
Porosity, ε	0.97	0.37
Thermal conductivity, k^* (W/m K)	2.52	10.73
Permeability, K (m^2)	2.50×10^{-7}	2.83×10^{-10}
Inertial coefficient, F	0.142	0.239

Twelve OMEGA T-TT-30 thermocouples were distributed on the heated side. As displayed in Fig. 3, the local temperatures of the conductive pipe and the aluminum foam regions on the heated side were monitored. Three additional thermocouples were employed to monitor the ambient temperature, the air temperature at the channel inlet and the air temperature at the channel outlet. A total of 15 thermocouples were connected to the data logger (YOKOGAWA DA100). All the temperature data printed out using the data recorder were then inputted into the computer and transformed into data for further analysis. The inlet air temperature was around 25 °C. The temperature difference between the air at the inlet and that at the outlet was 12–23 °C. The maximum wall temperatures were around 80 °C in all tests. The system was assumed to be in a steady state when the temperature varied by less than

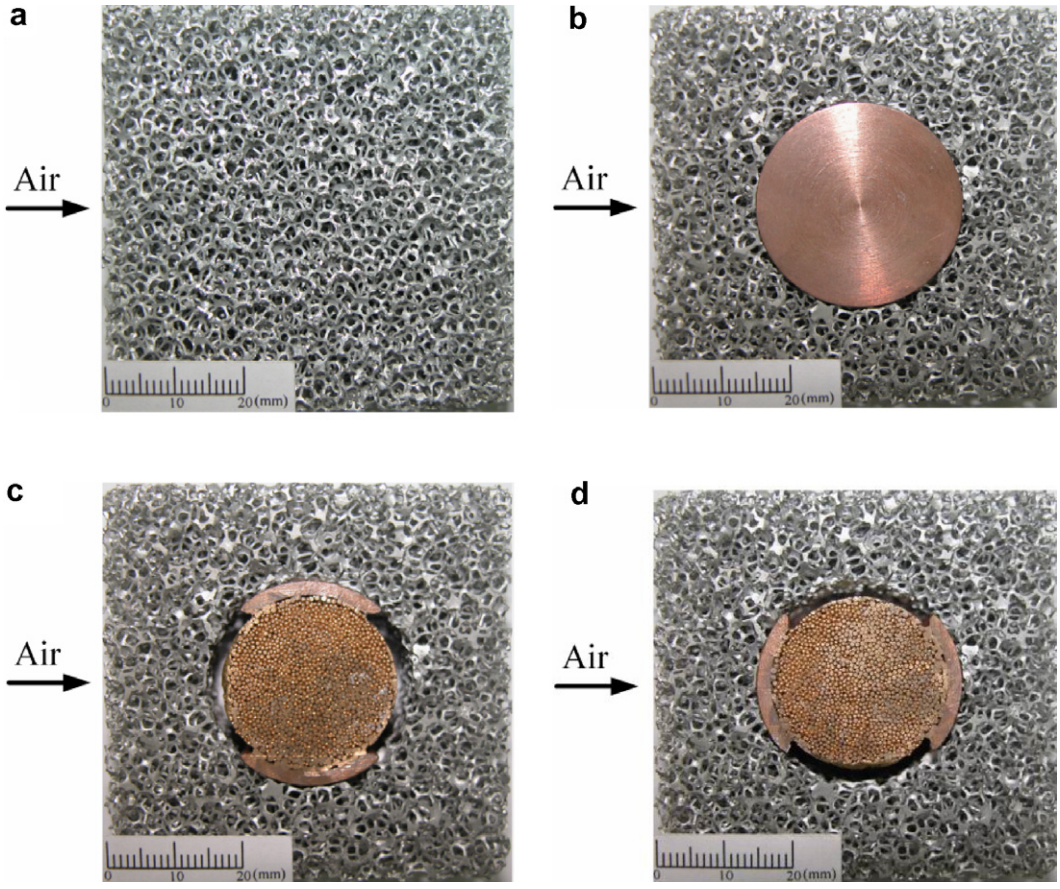

Fig. 2. Pictures of test specimens. (a) mode A, (b) mode B, (c) mode C and (d) mode D.

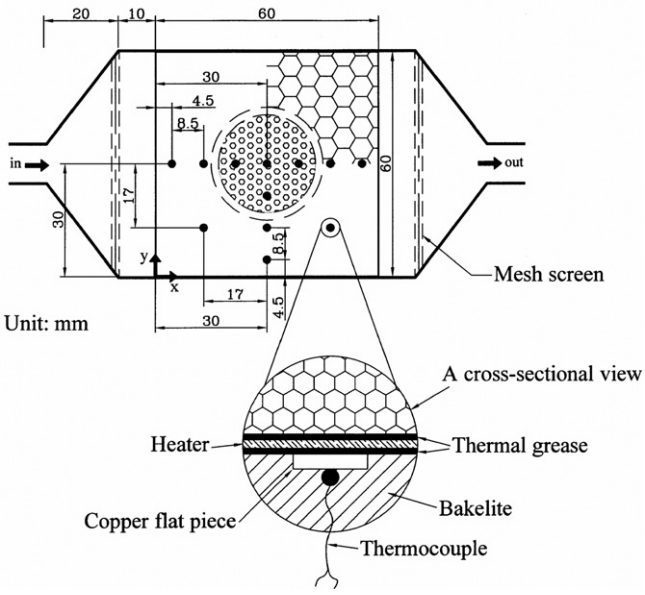

Fig. 3. Positions of thermocouple measured herein.

0.2 °C during a 15 min interval. Finally, the drop in pressure through each test specimen was determined using pressure transmitters (Kanomax, Model 6112, 0–5 kPa; Dwyer, Model MM1-E43B, 0–1 inch-H_2O).

3. Data reduction and uncertainty analysis

Measured fluid velocities, pressure drops and temperatures were used to determine the Reynolds numbers, the non-dimensional pressure drops and the local Nusselt numbers, using,

$$Re = \frac{\rho_f U H}{\mu} \tag{1}$$

$$P = \frac{p_i - p_e}{0.5\rho_f U^2} \tag{2}$$

$$Nu = \frac{qH}{(T_w - T_i)k_f} \tag{3}$$

where U is the average air velocity at the channel inlet; H is the height of the aluminum foam heat sink; p_i and p_e are the static pressures at the channel inlet and exit, respectively; T_w is the measured temperature of the bottom skin of the aluminum foam heat sink; T_i is the air temperature at the channel inlet, and q is the convective heat flux.

The maximum error in the flow rate and the pressure drop were ±5.0% and ±7.2% at 50 l/min, respectively. The inaccuracy in the recorder readings of temperature was ±0.2 °C. The extreme error in the heat balance due to heat loss was ±6.7%. The maximum errors in determining the channel height (H) and the fluid conductivity (k_f) were estimated to within ±1%. Uncertainties in parameters

were estimated using the root-sum-square method of Kline and McClintock [25] and Moffat [26]. The experimental data herein showed that the uncertainties in the Reynolds number, the non-dimensional pressure drop and the Nusselt number were ±5.6%, ±9.8% and ±7.1%, respectively.

4. Results and discussion

The work considers the spatial thermal regulation of an aluminum foam heat sink using a high-conductivity conductive pipe. Four test modes with various configurations of conductive pipes were used (as shown in Fig. 2). The range of Reynolds numbers was $Re = 883$–4416.

The validity of the experiments conducted herein is established by comparing the data concerning the aluminum foam heat sink without any conductive pipe (mode A), with that provided in the previous work. Fig. 4 plots the results of the comparison. The experimental data obtained by Calmidi and Mahajan [5], whose system was similar to that herein, were used. This figure depicts strong consistency between the data herein and those obtained by Calmidi and Mahajan [5], indicating that the measurements made herein are reasonable.

Fig. 5 represents the local Nusselt numbers (Nu) in the stream-wise direction along the centerline of the bottom surface of the heat sink. Fig. 5 also plots data for the system with a copper conductive pipe but no aluminum foam (as crosses). The figure reveals that the aluminum foams greatly improved cooling performance. Additionally, the aluminum foam heat sink with variously configured conductive pipes (in various test modes) exhibited different thermal behaviors. In mode A (the aluminum foam heat sink without any conductive pipe), Nu was a maximum at the channel inlet and slowly fell downstream. This finding is consistent with the heat transfer characteristics in a thermally developing channel flow. In mode B (the aluminum foam heat sink with a copper conductive pipe), the Nu was maximum in the conductive pipe region, as expected, because the high-conductivity conductive pipe embedded into the aluminum foams promoted heat transfer in the conductive pipe region. However, it also suppressed heat transfer upstream. In modes C and D (aluminum foam heat sinks with porous conductive pipes made of sintered bronze beads), the Nu distributions in the direction of the stream along the centerline of the bottom surface of the heat sink were quite interesting, and could perhaps be explained by the flow patterns that were caused by the interactions among the aluminum foam, the porous conductive pipe and the arc gap. In mode C (arc gaps at the front and rear of the copper shield of the porous conductive pipe), the arc gaps were designed to allow coolant to flow across the porous conductive pipe to carry heat away. However, the experimental results revealed that the Nu distribution was similar to that in mode A, indicating that the coolant was insufficient to enter the porous conductive pipe. This finding is reasonable because the permeability of the aluminum foams was 100 times that of the sintered bronze beads used herein. Accordingly, most of the coolant went through the aluminum foam regions adjacent to the conductive pipe. Moreover, the arc gaps at the front and at the rear of the copper shield of the porous conductive pipe prevented the heat from being transferred

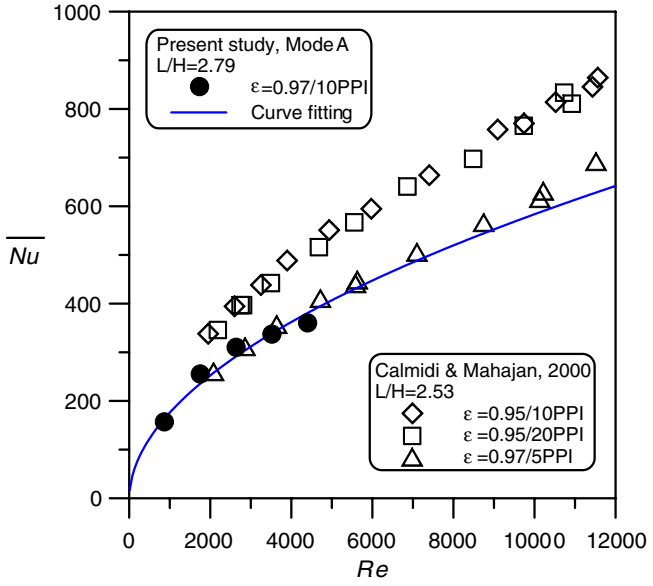

Fig. 4. Comparison with the other data Ref. [5] for the system without a conductive pipe.

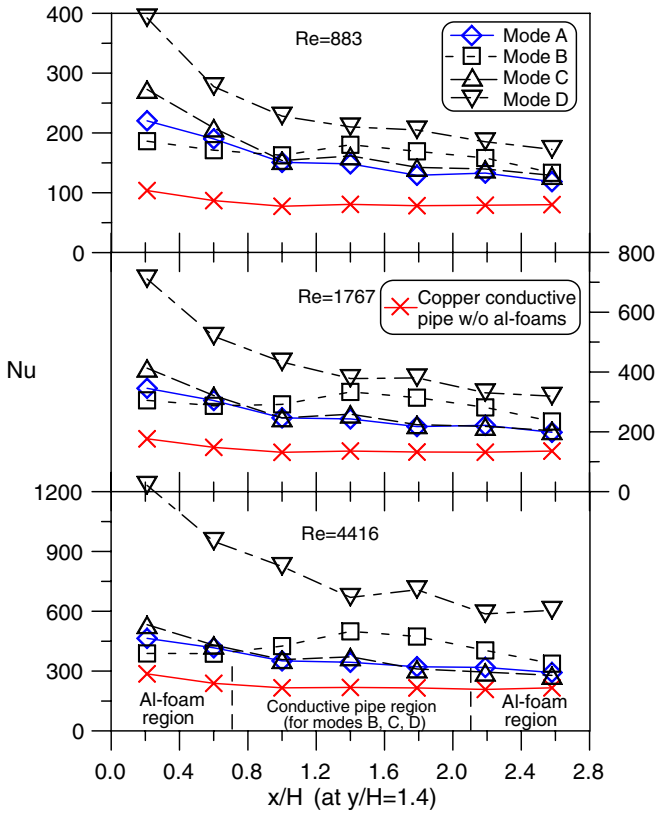

Fig. 5. Local Nusselt numbers in the stream-wise direction at $y/H = 1.4$.

upstream, weakening the effect of the conductive pipe on heat transfer. In mode D, the arc gaps were moved to the lateral sides of the porous conductive pipe. The experimental results indicate that the values of *Nu* in mode D greatly exceeded those in other modes, revealing that the coolant was concentrated in the center part of the heat sink by the lateral arc gaps because the flow resistance was small.

Fig. 6 displays the local Nusselt numbers (*Nu*) at $x/H = 1.4$. The results show that *Nu* in the conductive pipe region exceeded that in the aluminum foam region in the modes with conductive pipes. In mode A without a conductive pipe, the *Nu* distribution was smooth in the span-wise direction. In the conductive pipe region, the heat transfer was greatest in mode D and least in mode C, suggesting again that the arc gaps around the conductive pipe strongly affected the flow pattern through the aluminum heat sink. Notably, although the heat transfer in the conductive pipe region in mode D exceeded those in the other modes, the average heat transfer at $x/H = 1.4$ in mode D was not the greatest, because the heat transfer in the aluminum foam region in mode D was much lower than those in the other modes.

Fig. 7 shows the local Nusselt number distributions at various x positions in the system with a copper conductive pipe and without aluminum foam. These data defined the baseline, and showed that the *Nu* distribution at $x/H = 1.4$ in this system (on the middle line through the conductive pipe region) was similar to those at $x/H = 0.6$ and 2.2 (on the lines in front of and behind the conductive pipe region, respectively). These *Nu* values exhibited hill-shaped distributions. *Nu* was highest on the centerline of the heat sink, which finding is explained as follows. With regard to the *Nu* distribution at $x/H = 0.6$, the impinging effect increased the *Nu* on the centerline of the heat sink. With respect to the *Nu* distribution at $x/H = 1.4$, the conductive pipe increased the *Nu* along the centerline of the heat sink. Besides, through the convergence of the test section at the exit (as shown in Fig. 3), air flows next to the conductive pipe flowed together to be a combined flow. Therefore, at $x/H = 2.2$, this combined flow increased *Nu* on the centerline of the heat sink.

Fig. 8 presents the local Nusselt number distributions at various x values in various test modes. The data indicate that each mode was associated with its unique *Nu* distribution in the span-wise direction. In mode A, the *Nu* distributions were smooth in the span-wise direction at various x values. In mode B, the *Nu* distributions were shaped like hills in the span-wise direction at various x values. In mode C, the *Nu* values were distributed like hills in the span-wise direction at $x/H = 0.6$ and 1.4, but the distribution was concave at $x/H = 2.2$, because the aluminum foams stopped the air flows next to the conductive pipe combining together, decreasing convective heat transfer behind the conductive pipe. Furthermore, the arc gap in the rear of the copper shield of the porous conductive pipe also pre-

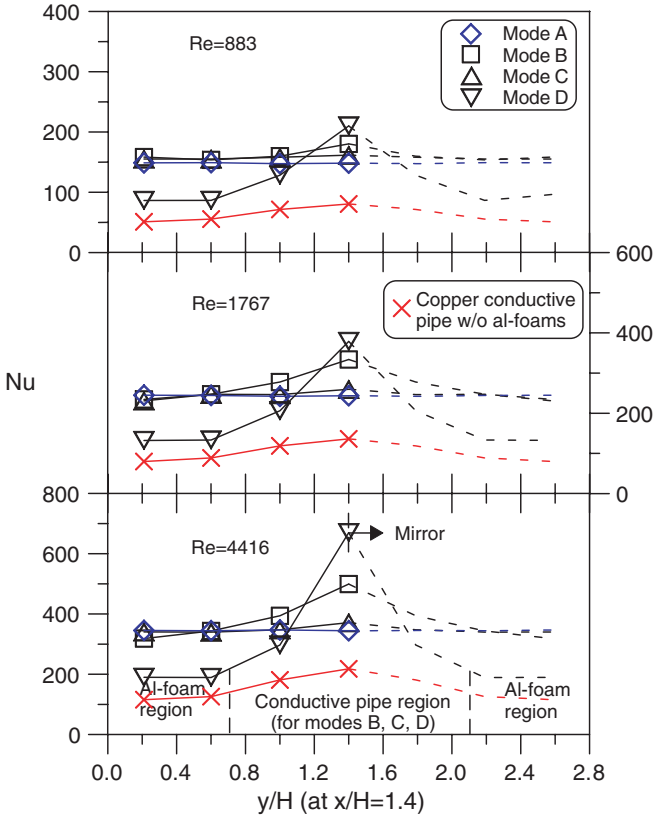

Fig. 6. Local Nusselt numbers in the span-wise direction at $x/H = 1.4$.

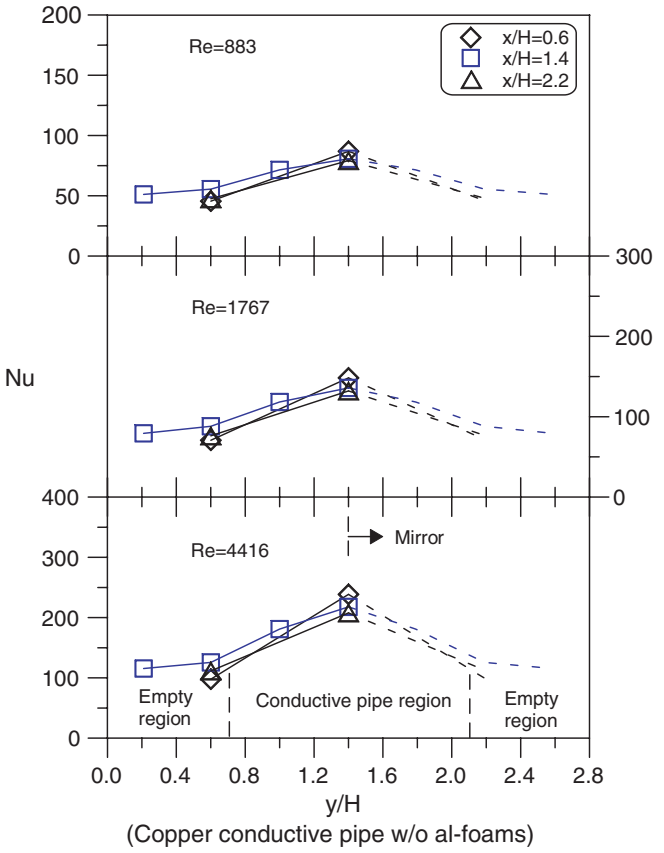

Fig. 7. Local Nusselt numbers in the span-wise direction for various x locations. (Copper conductive pipe without Al-foams.)

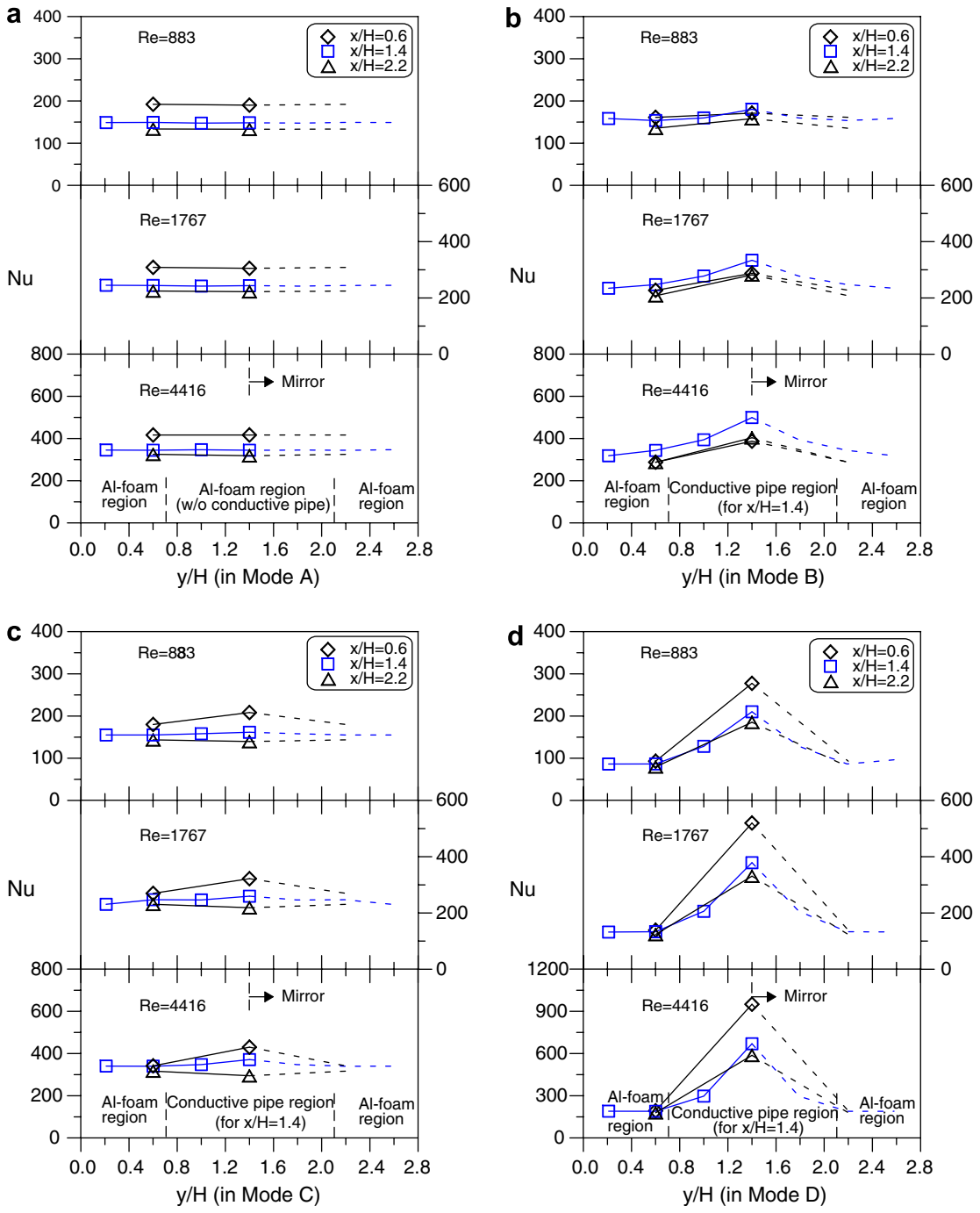

Fig. 8. Local Nusselt numbers in the span-wise direction for various x locations. (a) Mode A, (b) mode B, (c) mode C and (d) mode D.

venting the upstream transfer of the heat behind the conductive pipe. In mode D, the Nu values were distributed in the shape of high-mountains in the span-wise direction at various x values, because the lateral arc gaps strongly caused the coolant to concentrate at the center of the heat sink. Additionally, the upstream Nu was higher in all modes except in mode B, in which the Nu on the middle line across the conductive pipe region ($x/H = 1.4$) was greatest. In Figs. 5–8, the local Nusselt number distributions reveal that the effect of the modes on the spatial thermal regulation was very strong.

Fig. 9 plots the average Nusselt number against the Reynolds number in various test modes. Two average Nusselt numbers were used. One was the average Nusselt number ($\overline{Nu}_{(y/H=1.4)}$) at the centerline of the heat sink, and the other was the average Nusselt number ($\overline{Nu}$) over the whole heat sink. The definitions were expressed as follows:

$$\overline{Nu}_{(y/H=1.4)} = \left(\sum_{j=1}^{7} \frac{qH}{(T_{w,(y/H=1.4)} - T_i)_j k_f} \Delta x_j \right) \Big/ L, \tag{4}$$

$$\overline{Nu} = \overline{Nu}_{(y/H=1.4)} \frac{\overline{Nu}_{(x/H=1.4)}}{Nu_{(x/H=y/H=1.4)}}, \tag{5}$$

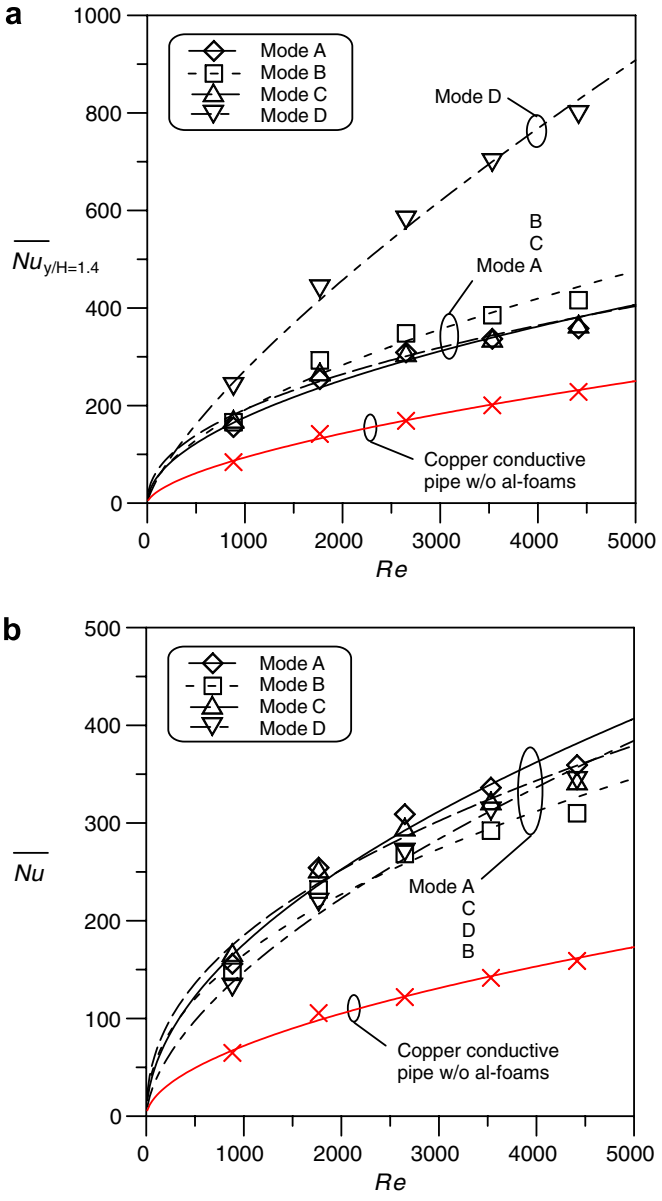

Fig. 9. Average Nusselt number as a function of Reynolds number. (a) Average Nusselt number at the centerline of the heat sink and (b) average Nusselt number for the whole heat sink.

where $\overline{Nu}_{(x/H=1.4)}$ is the average Nusselt number at x/H=1.4; $Nu_{(x/H=y/H=1.4)}$ is the local Nusselt number at $x/H = y/H$=1.4; $T_{w,(y/H=1.4)}$ is the local wall temperature in the stream-wise direction at $y/H = 1.4$; Δx is the spacing between thermocouples, and L is the length of the aluminum foam heat sink. The experimental data in Fig. 9(a) indicate that the $\overline{Nu}_{(y/H=1.4)}$ in mode D greatly exceeded those in the other modes. However, as presented in Fig. 9(b), the conductive pipe did not increase the overall average Nusselt number ($\overline{Nu}$) in the aluminum foam heat sink, indicating that conductive pipe in a porous heat sink was important in spatial thermal regulation. According to the experimental data, the relationship between the average Nusselt number ($\overline{Nu}_{(y/H=1.4)}$ or $\overline{Nu}$) and Re was given by

Table 2
The corresponding factors of correlation on the Nusselt numbers

	Mode A	Mode B	Mode C	Mode D
$\overline{Nu}_{(y/H=1.4)} = m_1 Re^{n_1}$				
m_1	4.832	3.821	7.885	1.544
n_1	0.520	0.566	0.462	0.749
$\overline{Nu} = m_2 Re^{n_2}$				
m_2	4.835	6.965	8.522	2.436
n_2	0.520	0.458	0.446	0.594

$$\overline{Nu}_{(y/H=1.4)} = m_1 Re^{n_1}, \tag{6}$$

$$\overline{Nu} = m_2 Re^{n_2}. \tag{7}$$

Table 2 lists the coefficients m_1, n_1, m_2 and n_2 in various test modes. The average deviation in Eqs. (6) and (7) was under 3%.

Two important characteristics – heat transfer performance and pressure drop – are investigated by conducting experiments on fluid flow and heat transfer. The experimental results presented in the preceding paragraphs clearly show that the conductive pipe used herein spatially regulated the heat transfer performance of the aluminum foam heat sink. The drop in pressure through each aluminum foam heat sink with variously configured conductive pipes was also examined. Fig. 10 plots the non-dimensional pressure drop (P) against the Reynolds number in various test modes. The figure reveals that the non-dimensional pressure drop declines as Re increases. It also indicates that conductive pipe increased the flow resistance in the aluminum foam heat sink. However, the lateral arc gaps, which were approximately along the stream-wise axis, clearly reduced the flow resistance in mode D below those in the other modes with conductive pipes. The open symbols plot

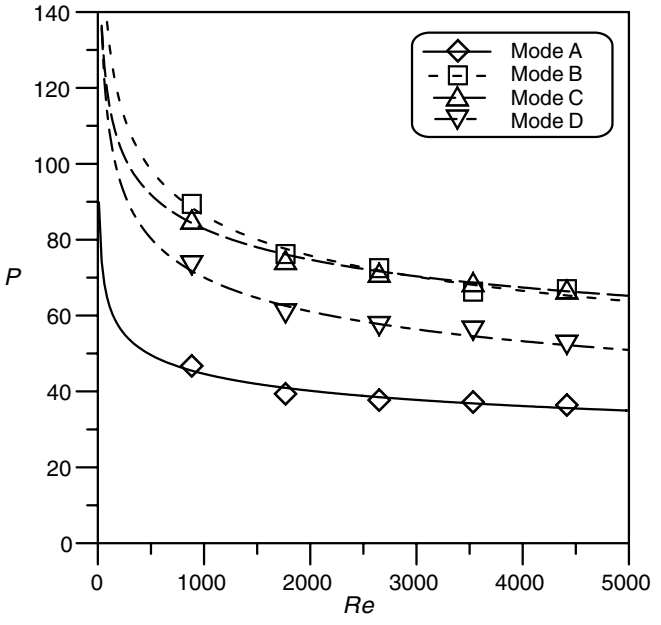

Fig. 10. Non-dimensional pressure drop as a function of Reynolds number.

the data obtained in various test modes; the lines that pass through these symbols are least-square fits. The basic correlation function is:

$$P = aRe^b. \tag{8}$$

Table 3 presents the coefficients a and b in various test modes. The average deviation between the experimental data and those obtained by Eq. (8) is under 3%. Additionally, a dimensionless pumping power (PRe^3) is introduced to evaluate the heat transfer performance in various test modes. Fig. 11 plots the relationship between the average Nusselt number ($\overline{Nu}_{(y/H=1.4)}$ or $\overline{Nu}$) and PRe^3, as determined using Eqs. (6)–(8). The results in Fig. 11(a) show that the $\overline{Nu}_{(y/H=1.4)}$ in mode D significantly exceeded those in the other modes at the same pumping power, suggesting the effectiveness of lateral arc gaps in spatial thermal regulation. However, the overall average Nusselt number ($\overline{Nu}$) was greatest in mode A (the system without a conductive pipe) and least in mode B (the system with the copper conductive pipe) for a particular pumping power. This finding demonstrates that the conductive pipe embedded in the aluminum heat sink did not promote overall heat transfer.

Table 3
The corresponding factors of correlation on the non-dimensional pressure drops

	Mode A	Mode B	Mode C	Mode D
$P = aRe^b$				
a	127.5	317.5	231.7	274.2
b	−0.152	−0.188	−0.149	−0.198

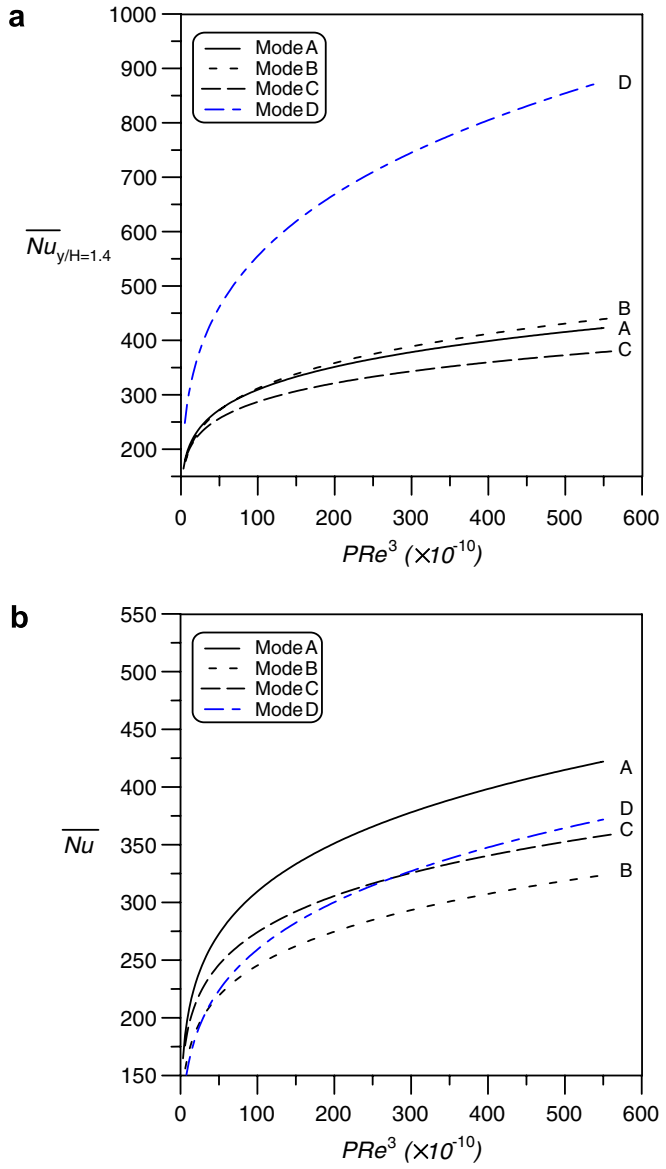

Fig. 11. Average Nusselt number as a function of non-dimensional pumping power. (a) Average Nusselt number at the centerline of the heat sink and (b) average Nusselt number for the whole heat sink.

5. Conclusion

The work investigated the spatial thermal regulation of an aluminum foam heat sink using a high-conductivity conductive pipe. The fluid medium was air. Four test modes with various configurations of the conductive pipes were considered. The range of Reynolds numbers was $Re = 883$–4416. The results indicate that the conductive pipe in a porous heat sink was very useful in spatial thermal regulation, especially in the test mode with the lateral arc gaps, which were roughly parallel to the stream-wise axis, adjacent to the conductive pipe. However, the conductive pipe in the aluminum foam heat sink studied herein, did not improve overall heat transfer.

Acknowledgements

The author would like to thank the National Science Council of the Republic of China for financially supporting this research under Contract No. NSC 93-2622-E-270-003-CC3.

References

[1] M.L. Hunt, C.L. Tien, Effects of thermal dispersion on forced convection in fibrous media, Int. J. Heat Mass Transfer 31 (1988) 301–309.
[2] S.Y. Kim, B.H. Kang, J.H. Kim, Forced convection from aluminum foam materials in an asymmetrically heated channel, Int. J. Heat Mass Transfer 44 (2001) 1451–1454.
[3] D. Angirasa, Forced convective heat transfer in metallic fibrous materials, ASME J. Heat Transfer 124 (2002) 739–745.
[4] D. Angirasa, Experimental investigation of forced convection heat transfer augmentation with metallic fibrous materials, Int. J. Heat Mass Transfer 45 (2002) 919–922.
[5] V.V. Calmidi, R.L. Mahajan, Forced convection in high porosity metal foams, ASME J. Heat Transfer 122 (2000) 557–565.
[6] K. Boomsma, D. Poulikakos, F. Zwick, Metal foams as compact high performance heat exchangers, Mech. Mater. 35 (2003) 1161–1176.
[7] G.J. Hwang, C.H. Chao, Heat transfer measurement and analysis for sintered porous channels, J. Heat Transfer 116 (1994) 456–464.
[8] G.J. Hwang, C.C. Wu, C.H. Chao, Investigation of non-Darcian forced convection in an asymmetrically heated sintered porous channel, J. Heat Transfer 117 (1995) 725–732.

[9] G.P. Peterson, C.S. Chang, Two-phase heat dissipation utilizing porous-channels of high-conductivity material, J. Heat Transfer 120 (1998) 243–252.
[10] P.X. Jiang, M. Li, T.J. Lu, L. Yu, Z.P. Ren, Experimental research on convection heat transfer in sintered porous plate channels, Int. J. Heat Mass Transfer 47 (2004) 2085–2096.
[11] P.X. Jiang, M. Li, Y.C. Ma, Z.P. Ren, Boundary conditions and wall effect for forced convection heat transfer in sintered porous plate channels, Int. J. Heat Mass Transfer 47 (2004) 2073–2083.
[12] T.A. Rizk, C. Kleinstreuer, Forced convective cooling of a linear array of blocks in open and porous matrix channels, Heat Transfer Eng. 12 (1991) 40–47.
[13] Y. Ould-Amer, S. Chikh, K. Bouhadef, G. Lauriat, Forced convection cooling enhancement by use of porous material, Int. J. Heat Fluid Flow 19 (1998) 251–258.
[14] P.C. Huang, C.F. Yang, J.J. Hwang, M.T. Chiu, Enhancement of forced-convection cooling of multiple heated blocks in a channel using porous covers, Int. J. Heat Mass Transfer 48 (2005) 647–664.
[15] A. Bhattacharya, R.L. Mahajan, Finned metal foam heat sinks for electronics cooling in forced convection, ASME J. Electron. Packaging 124 (2002) 155–163.
[16] S.C. Tzeng, T.M. Jeng, Y.C. Wang, Experimental study of forced convection in asymmetrically heated sintered porous channels with/without periodical baffles, Int. J. Heat Mass Transfer 49 (2006) 78–88.
[17] W.S. Fu, H.C. Huang, Thermal performances of different shape porous blocks under an impinging jet, Int. J. Heat Mass Transfer 40 (1997) 2261–2272.
[18] W.S. Fu, H.C. Huang, Effects of a random porosity model on heat transfer performance of porous media, Int. J. Heat Mass Transfer 42 (1999) 13–25.
[19] T.M. Jeng, S.C. Tzeng, Numerical study of confined slot jet impinging on porous metallic foam heat sink, Int. J. Heat Mass Transfer 48 (2005) 4685–4694.
[20] S.C. Tzeng, T.M. Jeng, Convective heat transfer in porous channels with 90° turned flow, Int. J. Heat Mass Transfer 49 (2006) 1452–1461.
[21] H.L. Fu, K.C. Leong, X.Y. Huang, C.Y. Liu, An experimental study of heat transfer of a porous channel subjected to oscillating flow, ASME J. Heat Transfer 123 (2001) 162–170.
[22] K.C. Leong, L.W. Jin, Heat transfer of oscillating and steady flows in a channel filled with porous media, Int. Commun. Heat Mass Transfer 31 (2004) 63–72.
[23] K.C. Leong, L.W. Jin, An experimental study of heat transfer in oscillating flow through a channel filled with an aluminum foam, Int. J. Heat Mass Transfer 48 (2005) 243–253.
[24] V.V. Calmidi, R.L. Mahajan, The effective thermal conductivity of high porosity fibrous metal foams, ASME J. Heat Transfer 121 (1999) 466–471.
[25] S.J. Kline, F.A. Mcclintock, Describing uncertainties in single-sample experiments, Mech. Eng. (1953) 3–8.
[26] R.J. Moffat, Contributions to the theory of single-sample uncertainty analysis, ASME J. Fluids Eng. 104 (1986) 250–260.